Analysis of metastatic-repressing microRNAs and determining *ZEB1* as a gene candidate for siRNA knockout in mesenchymal-like ovarian and prostate cancer cell lines

A Thesis

Presented to

The Academic Faculty

In Partial Fulfillment

Of the Requirements for the Degree

Bachelors of Science in the

School of Biological Sciences

Georgia Institute of Technology

Spring 2018

Analysis of metastatic-repressing microRNAs and determining *ZEB1* as a gene candidate for siRNA knockout in mesenchymal-like ovarian and prostate cancer cell lines

Approved By:

Dr. John McDonald, Advisor

School of Biological Sciences

Georgia Institute of Technology

Dr. Fredrik Vannberg

School of Biological Sciences

Georgia Institute of Technology

Date Approved: May 2, 2018

Table of Contents

ABSTRACT

MicroRNAs (miRNAs) have been shown to play a significant role in cancer progression and metastasis through their regulation of gene expression to activate epithelial-mesenchymal transition (EMT). Understanding the genetic and molecular basis for how microRNAs induce EMT's reciprocal mechanism, mesenchymal-epithelial transition (MET), is vital as metastatic disease is highly lethal. This study aims to identify genes involved in MET across two cancer types based on microRNA overexpressions that have previously been shown to induce MET in mesenchymal-like ovarian or prostate cancer cell lines. It also aims to understand how the same microRNAs behave in similar mesenchymal cell-lines. To elucidate the ability of different microRNAs to induce the same process of MET in two reproductive cancer cell lines, transfections to overexpress miR-429, miR-203a, and miR-205 in both ovarian cancer and prostate cancer cell lines, HEY and PC3, respectively, were performed. Using microarray analysis, differentially expressed genes were identified and comparisons of these genes to known EMT/MET genes was done to narrow down a set of genes important in both ovarian and prostate cancer MET processes. We show that miR-429 induces MET in both HEY and PC3 cells, but not through similar pathways, and that overexpression of miR-203a and miR-205 induced MET in either HEY or PC3, but not both. *ZEB1* was identified as a gene candidate for siRNA knockout to recapitulate MET and further elucidate mechanisms of the three microRNAs inducing MET.

INTRODUCTION

Ovarian cancer is highly metastatic and is the most lethal of gynecologic cancers [1]. Prostate cancer is also the most lethal of the male reproductive system cancers and is the second-leading cause of cancer-related deaths in males. Survival rates of later stages of metastatic ovarian and prostate cancer are markedly lower than when they are detected in their earlier stages. The lethality of these more advanced cancers lies in their highly metastatic nature. Current chemotherapies, radiation therapies, and surgeries are not guaranteed to treat every location of disease in the body, which increases the possibility of recurrence of the cancer.

The processes underlying metastasis manifest differently in diverse cancer types, and each has varying locations of metastases in the body [13]. This holds true for prostate and ovarian cancer as well, where prostate cancer metastasizes strongly to the bone, and ovarian cancer metastasizes primarily to the abdominal cavity [13, 14]. Nevertheless, an underlying cellular mechanism by which primary tumor cells of both cancers undergo metastasis is known as epithelial-to-mesenchymal transition (EMT) [2]. During EMT, the intercellular adhesions of epithelial cells are disrupted, the cells become less proliferative, and the cells become more motile and invasive by becoming more mesenchymal-like before intravasation in metastasis [3]. Phenotypically, epithelial cells are characterized by a cuboidal shape, while mesenchymal cells are longer and thinner, thus allowing for greater motility. Upon arrival to the secondary tumor site, the cells revert to the epithelial state by undergoing mesenchymal-to-epithelial transition (MET). Inducing MET in a mesenchymal cell reverses the EMT process and could create an environment for the tumor to be more sensitive to current chemotherapies such as cisplatin

that target epithelial cell types. The specific mechanisms by which EMT/MET occurs in prostate and ovarian cancer cells have been shown to be different with respect to each cancer type [15,16]. However, an underlying factor shared by many cancer types is the multitude of roles microRNAs have been shown to play in cancer progression [17]. One such role is the involvement of members of the miR-200 family of microRNAs in a double-negative feedback loop with *ZEB1* and *ZEB2* to initiate EMT [18]. This double-negative feedback loop is a process shared by multiple cancer types, which may show similar involvements for the same miRNA in multiple cancer types [18].

MicroRNAs (miRNA) are short, non-coding RNAs involved in the regulation of gene expression by either translational repression or degradation of target messenger RNAs (mRNAs), and have been shown to contribute to cancer development through their role of up regulating or down regulating different genes through loss and gain of miRNA function, respectively [4]. MicroRNAs can also be involved in the post-transcriptional regulation of mRNA, thus affecting protein level independently of the varying mRNA expression seen in cancer development [8]. Due to the highly conserved seed regions of microRNAs, which bind to the 3'-untranslated region (UTR) of their target mRNAs, a single microRNA can regulate many gene targets simultaneously, making these small RNAs a useful regulator of gene expression [9]. This endogenous regulation of multiple genes at once by a single miRNA presents an opportunity to further explore the effects of a single microRNA on multiple types of cancer, and specifically, if a single microRNA can induce the same processes, such as mesenchymal-epithelial transition (MET) across diverse types of cancer.

Previous studies have established the role of various microRNAs in a miRNA-mediated regulatory pathway that influences MET. An example is the overexpression of miR-429, a member of the miR-200 family that contributes to the induction of MET in metastatic ovarian cancer cells (HEY) [5]. Overexpression of miR-203 has been shown to induce MET in metastatic prostate cancer cells (PC3) [6]. It has also been reported that miR-205 is a tumor suppressor in prostate cancer that targets c-SRC, and overexpression of it in PC3 cells lessened cell proliferation, invasion, and tumor growth [7]. These microRNAs seem to induce similar phenotypic changes conducive with MET in varying cell lines. However, while previous studies have looked at these microRNAs in the context of a single cell line of interest and shown that they induce MET, they have not explored the effects of the same microRNA in a different cancer cell line. Doing so may show some overlap in the underlying MET mechanisms across different metastatic cell types, in this case, prostate and ovarian cancer, because microRNAs have multiple gene targets. This endogenous characteristic of microRNAs having multiple gene targets makes it possible that there may be some overlap in a single microRNA's gene targets that induce MET in multiple cell lines. Identifying what common gene targets are shared by a single microRNA that induces MET in different cancer cell lines presents an opportunity to develop a better biomarker or therapeutic agent to treat a broad range of cancers in the future, as well as elucidate an underlying mechanism that multiple cancers share in the induction of MET.

This study, by overexpressing miR-429, miR-203a, and miR-205 in ovarian cancer and prostate cancer cells, aims to explore the genetic and molecular basis for EMT/MET in the two mesenchymal-like cell lines, HEY and PC3. We have been able to induce MET using the same

microRNA, miR-429, in both HEY and PC3 cells, and we have been able to identify trends in differential expression of genes induced with the three microRNAs of interest. We have also been able to identify *ZEB1* as a gene candidate for future short-interfering RNA (siRNA) knockout as it is implicated in inducing MET in both cell lines and is a target of all three microRNAs. SiRNA knockout of *ZEB1* will be done in future work to postulate a mechanism of action for MET in both cell lines as well as to gain an understanding of *ZEB1*'s direct and indirect effects in the setting of MET on both mesenchymal-like cell lines. Short-interfering RNAs are like microRNAs in that they induce mRNA degradation or silencing, but where miRNAs are naturally occurring nucleic acids that typically target hundreds of genes, siRNAs are designed and synthesized to target a single gene. Successful siRNA knockout of these candidate genes determined in this study could eventually lead to the development of versatile therapeutic agents for a wide range of cancers as well as a better understanding of MET in multiple types of cancer.

METHODS

This experiment was conducted by overexpressing miR-429, miR-203a, and miR-205 in mesenchymal-like ovarian and prostate cancer cell lines to observe differences in MET induction between the two cell lines transfected with different microRNAs. These observations were addressed objectively using CellProfiler to deduce the samples that induced MET. Microarray analysis was used to determine differentially expressed genes. These genes were compared against putative direct miRNA targets of miR-429, miR-203a, and miR-205 to

determine possible direct/indirect relationships between the gene expression inducing MET and its respective microRNA. The results of the microarray analysis of differentially expressed genes between treatments was also used to further elucidate important genes involved in MET that may be candidates for future siRNA (short-interfering RNA) knockout.

Transfection

The cell lines used for this experiment were HEY and PC3, a mesenchymal-like human ovarian and prostate cancer cell line, respectively. To perform the transfection of the HEY and PC3 cells with miR-429, miR-203a, and miR-205, each combination of HEY and PC3 with the three miRNAs was done in a separate 12-well plate, for a total of six treatments. For each transfection experiment, the 12-well plate was seeded with an appropriate number of cells: 40,000 cells/well for PC3 and 25,000 cells/well for HEY. The number of cells for each cell line was different because HEY cells grow better in smaller numbers than PC3 cells do. Nine wells were seeded with the appropriate number of cells, and the last three cells contained PBS to balance the plate. The cells grew with complete RPMI 1640 media containing fetal bovine serum and antibiotics (known as R10 media) in 37°C until they reached their exponential phase of growth, at about 24 hours post-seeding. At the 24-hour

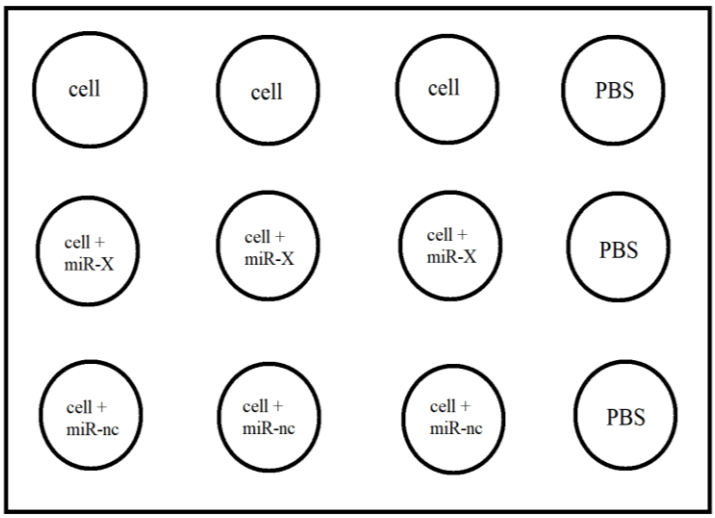

Figure 1: 12-well plate set-up. Cell includes either HEY or PC3 cells. MiR-X includes miR-429, miR-203a, or miR-205. MiR-NC is the negative control microRNA. PBS was used to balance the plate.

mark, the cells were transfected with the microRNA of interest (miR-429, miR-203a, and miR-205) and the negative control microRNA (miR-NC) using Lipofectamine 2000 and Opti-MEM media. The negative control samples were transfected with miR-NC, a negative control microRNA that does not target any genes that are targeted by miR-429, miR-203a, or miR-205, but is used to normalize the effect of transfecting cells with Lipofectamine 2000. Lipofectamine 2000 is the transfection reagent that allows the uptake of microRNA into the cell and Opti-MEM media contains reduced levels of fetal bovine serum, making transfection more effective. Three wells containing cells were transfected with the microRNA of interest and another three wells were transfected with miR-NC. Each well serves as a single replicate. The last three wells of cells were allowed to grow with no interference. Four hours after transfection, the Opti-Mem media was changed to R10 media, and the cells were left to incubate in 37°C for another 44 hours. At the 48-hour mark, pictures of the cells were taken and the cells were collected and frozen for future RNA extraction and microarray analysis. Each combination of cell type and microRNA of interest was transfected with a negative control in a separate 12-well plate.

Of note, the PC3 cells transfected with miR-429 sample, along with its own negative control sample, was repeated with two replicates for miR-429 and miR-NC, and included in the analysis with its own negative control separate from that of the other samples.

RNA Extraction

RNeasy Micro Kit (Qiagen, Germantown, MD) protocols were followed for RNA extraction from the HEY and PC3 cells. The RNA concentration was checked using Nanodrop Spectrophotometer (Thermo Fisher Scientific, Grand Island, NY). RNA quality for all samples

was verified using Agilent RNA 6000 Pico KIT for Bioanalyzer (Agilent Technologies, Santa Clara, CA). The RNA from the extractions was amplified with Applause 3'-Amp System (NuGEN Technologies, San Carlos, CA) and labeled with the Encore Biotin Module (NuGEN Technologies) to produce a cDNA suitable for hybridizing to GeneChip Human Genome U133 2.0 Array (Affymetrix, Santa Clara, CA) following manufacturers' recommendations.

Microarray Data Analysis

Gene expression for each sample was measured by microarray. Microarray analysis was done using the Affymetrix Human Genome U133 Plus 2.0 Array as previously described [10]. Twenty-five individual gene expression profiles were generated from the HEY and PC3 samples with miR-429, miR-203a, miR-205, and miR-NC. MiR-429 and miR-NC transfected into PC3 samples, there were two replicates for each microRNA. This gave a total of 5 expression profiles for miR-429 samples and eight expression profiles for the negative control samples. The 25 Affymetrix .CEL files were processed using the Affymetrix Expression Console (EC) Software Version 1.1 using the Robust Multi-Array Average (RMA) normalization method. The normalized expression values from all eight samples were $\log_2$ transformed.

The initial data contained 23,033 gene expression values from the Affymetrix Human Genome U133 Plus 2.0 chip. The $\log_2$-transformed expression values were averaged across the replicates for each combination of HEY or PC3 transfected with a single microRNA (i.e. HEY cells transfected with miR-429 or PC3 cells transfected with miR-NC). A two-tailed modified T-test ($p < 0.05$) was applied to identify genes that had significantly different expressions between the microRNA sample and negative control sample for each treatment. After determining

statistically significant expression values, the base two logarithm fold change ($\log_2$(FC)) of expression values was determined. The $\log_2$(FC) was calculated by subtracting the average negative control value from the average microRNA treatment value. Positive and negative $\log_2$(FC) values showed over-expression and under-expression of the gene, respectively. The 23,033 genes were then filtered based on statistically significant differential expression ($p < 0.05$) and a fold change ratio cutoff of 1.5. If $\log_2$(FC) values were greater than $\log_2$(1.5) or less than $-\log_2$(1.5), and statistically significant ($p < 0.05$), they were denoted to be differentially expressed (DE).

Analysis of microRNA putative direct targets with differentially expressed genes

The differential gene expression results were compared against putative direct targets of miR-429, miR-203(a), and miR-205 for each respective sample to determine how much of the effects of each microRNA are indirect or direct with respect to the other samples. The miRNA target data was retrieved from microrna.org (August 2010 release) [12].

RESULTS

miR-429, miR-203a, miR-205 and miR-NC overexpressed in HEY and PC3 samples

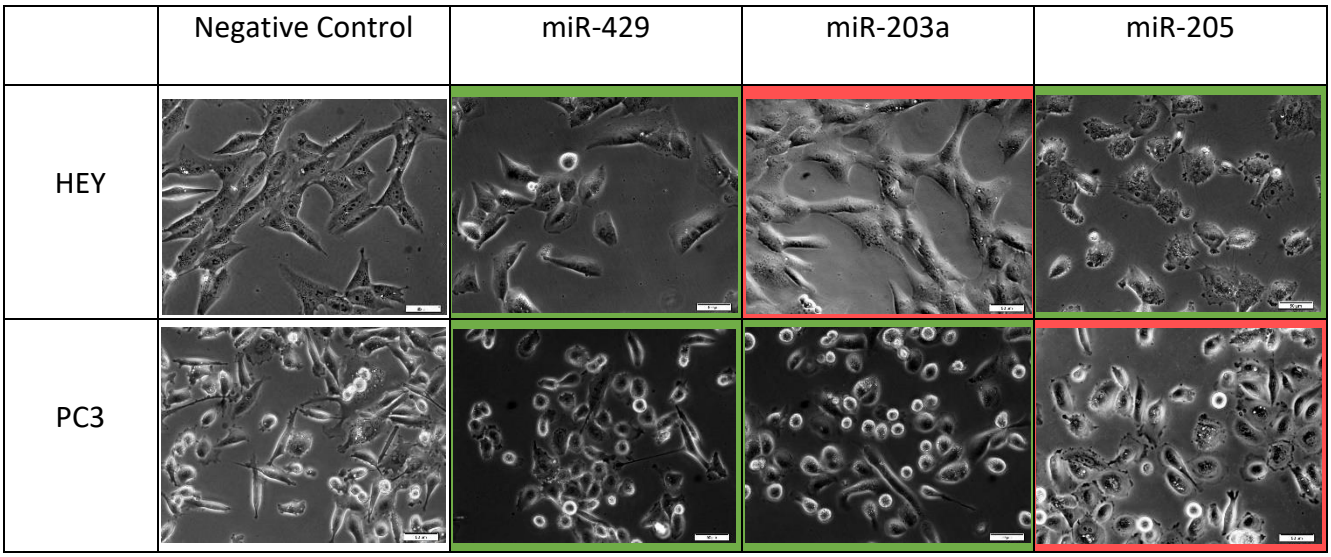

Figure 2: Overexpression of miR-429, miR-203a, miR-205, and miR-NC in HEY and PC3 cells (scale bar = 50 µm). Green boxes indicate treatments that induced MET (classified based on eccentricity values of treatments in Figure 3), and red boxes indicate treatments that did not induce MET.

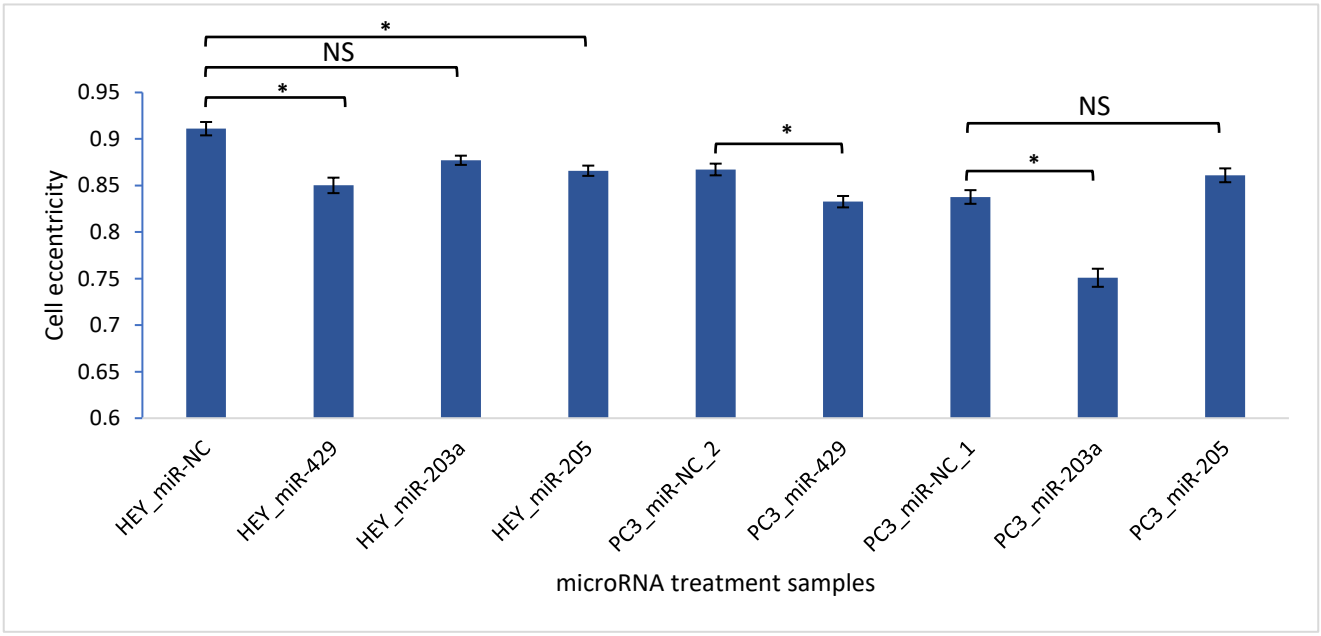

*Figure 3: Cell eccentricity values of transfected HEY and PC3 cells. Values represent mean ± SEM (n=251-544 cells analyzed per group). Asterisks represent significant differences from the negative control (*P< 0.0001, NS = not significant, Mann-Whitney U test).*

The initial transfection experiment with the three microRNAs and HEY and PC3 cells showed MET-like phenotypic changes in four treatments after 48 hours (Figure 2). The objective determination of MET occurring was done using an eccentricity comparison between the miRNA of interest-transfected treatment and its corresponding negative control, where a lower eccentricity value was expected for the treatments that induced MET. The eccentricity comparison was done using CellProfiler with images taken at 48 hours post-transfection (Figure 3). All eccentricity values of HEY samples treated with either miR-429, 203a, or 205 were compared against "HEY_miR-NC." PC3 samples had two negative controls, "PC3_miR-NC_1" and "PC3_miR-NC_2," the latter of which was used to compare against "PC3_miR-429" and the former of which was used against the PC3 cells overexpressed with miR-203a and miR-205 treatment. The treatments significant for a difference in eccentricity (Mann-Whitney U, $p < 0.0001$) were miR-429-overexpressed in HEY and PC3, miR-203a-overexpressed in PC3, and miR-205-overexpressed in HEY cells. These four treatments are identified as treatments that induce MET from this point forward. MiR-203a overexpressed in HEY cells and miR-205 in PC3 cells were not significantly different in eccentricity and therefore did not induce MET. Phenotypic observations from Figure 2 shows that HEY and PC3 cells transfected with miR-NC demonstrate the typical mesenchymal-like cell phenotype where the cell is elongated and have projections from the cell body. HEY and PC3 cells with miR-429 overexpressed, HEY cells with miR-205 overexpressed, and PC3 cells with miR-203a overexpressed exhibit less extreme elongation and are more cuboidal in shape, lacking strong projections from the cell bodies characteristic of mesenchymal-to-epithelial transition. The other treatments, miR-205 overexpressed in PC3 and miR-203a overexpressed in HEY, did not display phenotypic changes

characteristic of MET. For example, MiR-205 overexpressed in PC3 cells still exhibited long projections, indicative of the cell's motility as a mesenchymal cell [19]. MiR-203a overexpression in HEY cells also did not show a more cuboidal-shaped phenotype and showed strong projections in individual cells. The phenotypic subjective observations are consistent with the objective eccentricity analysis to identify miR-429 in HEY and PC3 cells, miR-203a in PC3 cells, and miR-205 in HEY cells as the treatments that induced MET.

During the initial transfection experiment, it is worth noting that transfection of PC3 cells was more difficult compared to HEY cells, because after 48-hours post transfection, more cells had died in the PC3 samples. This may be due to a higher sensitivity of PC3 cells to the transfection reagent, Lipofectamine 2000, which can exhibit cytotoxic effects on cells.

Each treatment showed differing amounts of differentially expressed genes

Differentially expressed genes were determined based on two criteria: two-tailed modified T-test (using R) evaluated at $p < 0.05$ and fold change (FC) ratio cutoff of 1.5 (Table 1). The number of differentially expressed genes is without regard to direction of expression. For the miR-429 samples, 7,179 and 1447 genes were differentially expressed for HEY and PC3, respectively. For miR-203a samples, 1,389 and 6,877 genes were differentially expressed for HEY and PC3, respectively. Lastly, for miR-205-overexpressed samples, 9,146 and 5,806 genes were differentially expressed for HEY and PC3.

	HEY	PC3
miR-429	7179	1447
miR-203a	1389	6877
miR-205	9146	5806

Table 1: Number of differentially expressed (DE) genes after 48-hour transfection of microRNAs. Criteria for DE: P < 0.05, FC = 1.5.

Comparison of direct putative miRNA targets with differentially expressed genes

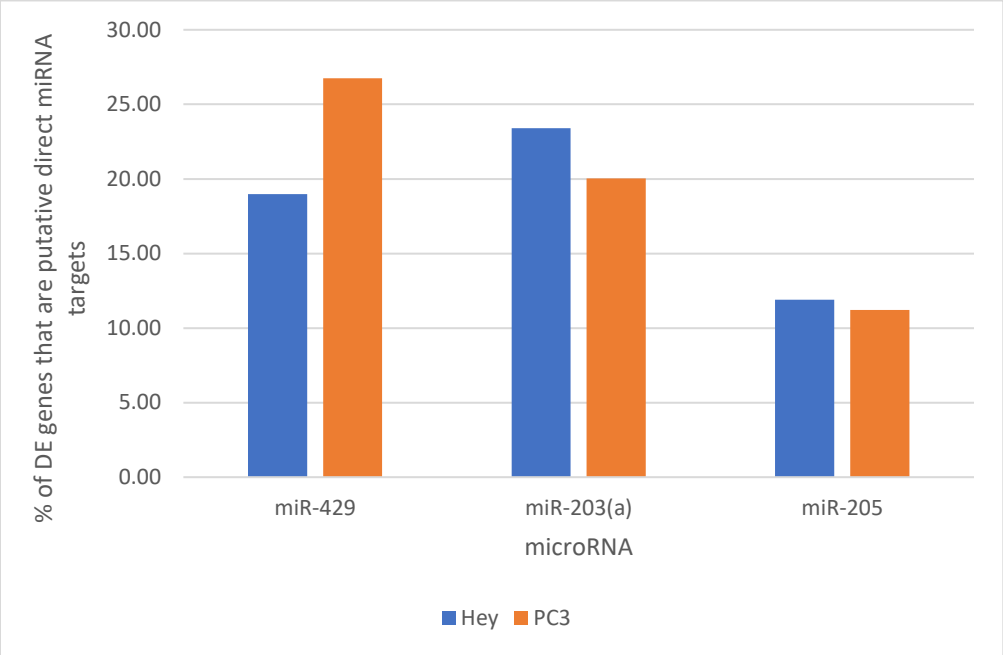

Figure 4: Percentage of differentially expressed genes that are putative direct targets of their respective microRNA (miR-429, miR-203a, and miR-205)

The number of putative direct targets obtained from microrna.org for miR-429, miR-203a, and miR-205, were 4141, 5345, and 2941 genes, respectively. For miR-429, these 4,141 genes were compared against the 7,179 DE genes in HEY and 1,447 DE genes in PC3. The same was done for the respective number of direct targets of miR-203a and miR-205 with their transfected HEY and PC3 samples (Figure 4). Of the 7,179 DE genes resulting from miR-429 transfected in HEY, 19% are putative direct targets of miR-429. For PC3 transfected with HEY, 27% of the 1,447 genes are direct putative gene targets of miR-429. For HEY and PC3 transfected with miR-203a, 23% and 20% of the differentially expressed genes are putative direct targets of miR-203a, respectively. For HEY and PC3 cells transfected with miR-205, 12% and 11% of the differentially expressed genes are putative targets of miR-205, respectively.

Finding MET-implicated genes across all treatments that induced MET

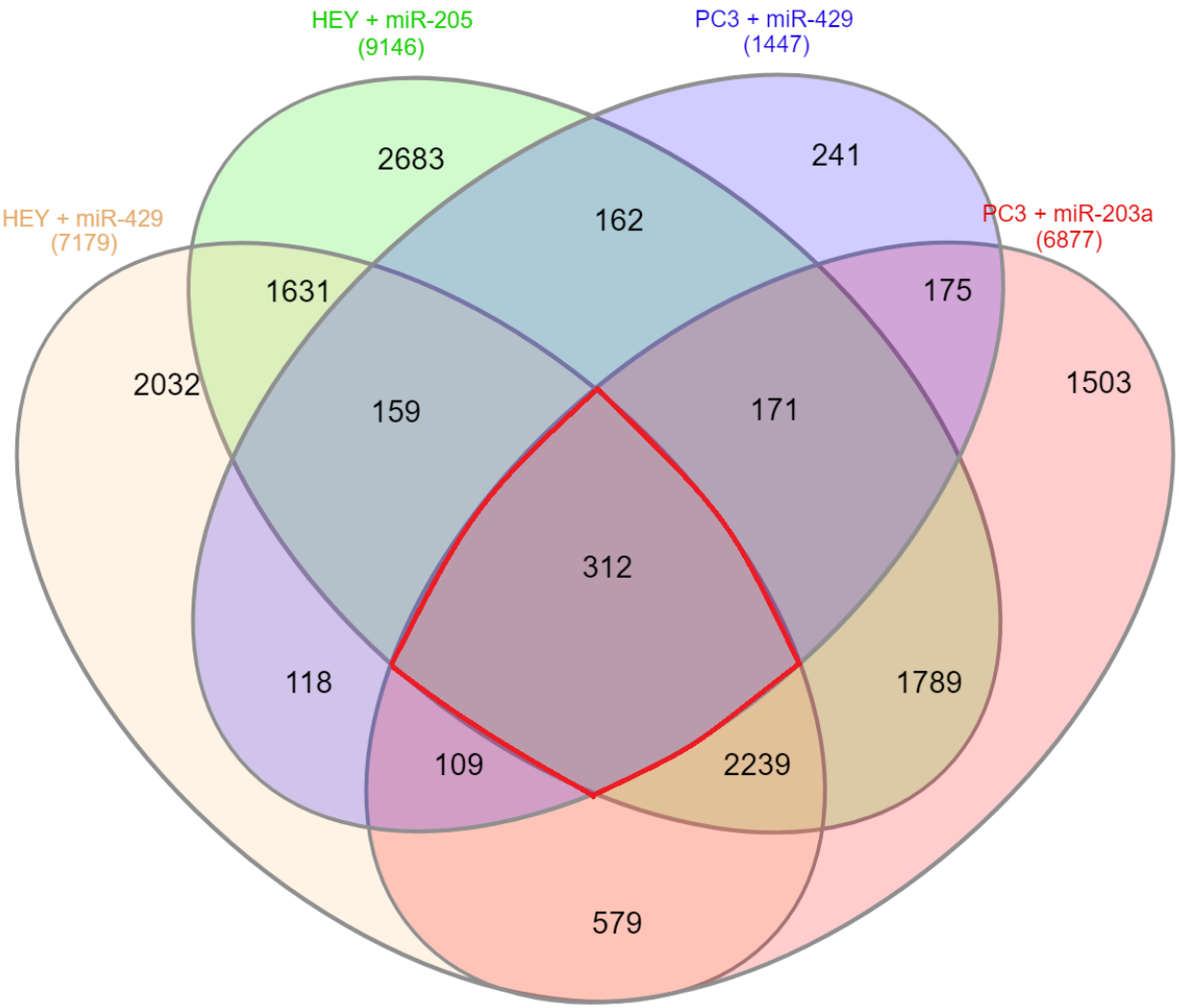

Figure 5: Venn diagram comparisons of DE genes between samples which showed MET. Numbers in parenthesis are the number of DE genes for each treatment included in the venn diagram comparisons. Section outlined in red with 312 genes is most common list of MET-implicated genes among the four samples.

After determining which treatments induced changes characteristic of MET and determining the number of differentially expressed (DE) genes in each, the DE genes between these samples were compared to find genes in common that may be implicated in MET. To filter the DE genes to find those that may be implicated in MET across both cell lines, a series of Venn-diagram comparisons and their intersections of genes found to be in common were made

between the four microRNA treatments that induced MET (Figure 5). There were 698 genes in common between the HEY and PC3 cells that were both treated with miR-429. Between both HEY samples that showed MET (miR-429 and miR-205) they shared 4,341 genes. The two PC3 samples that demonstrated MET (miR-429 and miR-203a) shared 767 genes. There were 312 genes (outlined in red) which are the most specific set of genes because of the induction of MET in the cells. These 312 genes are the result of all the treatments that showed MET. From these 312 genes, henceforth denoted "312 MET genes" we can further deduce what genes can be candidates for siRNA knockdown.

Narrowing down the 312 MET gene list to identify potential siRNA knockdown candidates

Gene	miRNA target	PC3-203a		HEY-205		HEY-429		PC3-429	
		logFC	p value	logFC	p value	logFC	p value	logFC	p value
GNG11	-	-1.398	1.15E-08	-1.642	5.98E-10	-1.282	5.22E-08	-0.851	2.50E-05
TCF4	miR-203a	-0.847	1.13E-07	-1.288	5.17E-11	-0.866	7.78E-08	-0.844	1.21E-07
WNT5A	miR-429, 205	-1.017	8.51E-09	-1.834	7.29E-14	-1.033	6.36E-09	-0.646	1.14E-05
ZEB1	miR-429, 203a, 205	-1.185	1.71E-08	-1.877	2.51E-12	-1.974	8.86E-13	-1.094	6.87E-08

Table 2: Downregulated 312 MET genes confirmed in EMT literature list and potential siRNA candidates

After determining the 312 genes that are differentially expressed in all treatments that were involved in MET, we wanted to narrow down our gene list to those essential for MET. Once identified, subsequent siRNA knockdown can be employed to attempt to recapitulate the effect of MET from overexpression of the microRNAs in their respective cell lines. Attempting to recapitulate MET with siRNA knockdown will help elucidate a mechanism of action for the miRNAs inducing MET in the different cell lines. To identify the putative target genes, we compared the list of 312 genes to 84 genes from a literature-based EMT gene list from RT²

Profiler™ PCR Array Human Epithelial to Mesenchymal Transition (Qiagen) [20]. This comparison gave five genes in both gene lists: GNG11, KRT7, TCF4, WNT5A, and ZEB1. These genes, except for KRT7, were downregulated, and these are of interest since in recapitulation with siRNA knockdown, we would expect to see downregulation of the gene candidates (Table 3). ZEB1 was the only gene in the resulting four downregulated MET genes that was a target of all three microRNAs used in the experiment.

Pathway enrichment of all differentially expressed genes

To evaluate what pathways were enriched in each microRNA treatment sample, pathway enrichment analysis was performed using ToppGene (with an FDR correction $p < 0.05$) on each set of differentially expressed genes as well as on the 312 MET gene list. The top 50 pathway enrichments for each DE gene treatment based on p-value, and all shared pathways of the DE gene treatments and 312 MET genes are reported in Supplementary Tables (Appendix). The top five pathways enriched of 160 in the HEY+miR-429 treatment are gene expression, organelle biogenesis and maintenance, mitochondrial translation initiation, mitochondrial translation elongation, and mitochondrial translation (ST1, Appendix). The five pathways enriched in the HEY+miR-203a treatment are cytokine-cytokine receptor interaction, starch and sucrose metabolism, digestion of dietary carbohydrate, extracellular matrix organization, and rheumatoid arthritis (ST2, Appendix). The top five pathways of 255 enriched in the HEY + miR-205 are gene expression, metabolism, metabolic pathways, cell cycle (mitotic), and asparagine N-linked glycosylation (ST3, Appendix). For PC3+miR-429, the top five pathways enriched of 13

are cell junction organization, proteoglycans in cancer, cell-cell junction organization, Hippo signaling pathway, and pathways in cancer (ST4, Appendix). The top five pathways enriched of 261 for PC3+miR-203a are gene expression, metabolism of proteins, metabolism, rRNA processing in the nucleus and cytosol, and organelle biogenesis and maintenance (ST5, Appendix). The top five pathways enriched of 218 for PC3 + miR-205 are interferon alpha/beta signaling, gene expression, mitotic cell cycle, metabolism/metabolism of proteins, and ER-phagosome pathway (ST6, Appendix). The top five pathways of 136 that the 312 MET genes were enriched in were: IL23-mediated signaling events; PI3K-Akt signaling pathway; histidine, lysine, phenylalanine, tyrosine, proline, and tryptophan catabolism; hypoxia and p53 in the cardiovascular system; and the mTOR signaling pathway.

Many of the treatments shared pathway enrichments (ST8, Appendix). There were zero common pathways for the four MET-induced treatments, and when PC3+miR-429 was excluded, there were 94 common pathways between HEY+miR-429, HEY+miR-205, and PC3+miR-203a. When PC3+miR-205 was included with they MET-inducing HEY samples and PC3+miR-203a, there were 85 common pathway enrichments. Excluding any miR-429 treatments, when comparing PC3+miR-203a and HEY+miR-205 pathway enrichments, they shared 131 pathways. When comparing the miR-429 treatments, between the 161 pathway enrichments of HEY+miR-429 and 13 pathway enrichments of PC3+miR-429, there were no common enrichments. When comparing the miR-203a treatments, there was one pathway, extracellular matrix organization, that was shared between the six pathway enrichments of HEY+miR-203a and 260 enrichments of HEY+miR-203a. For the miR-205 treatments, there were

124 shared pathway enrichments between the 255 enrichments of HEY+miR-205 and 218 enrichments of PC3+miR-205.

DISCUSSION

In this study we demonstrate that the same microRNA (miR-429) can exhibit mesenchymal-to-epithelial transition in different cell lines that share phenotypic characteristics (HEY and PC3). By contrast, the two other microRNAs of interest in this study, miR-203a and miR-205, only induced MET in PC3 and HEY, respectively, but not both. We also demonstrate that for miR-203a and miR-205, the number of differentially expressed genes in each cell line is related to if MET was induced. The samples that did not induce MET (miR-203a+HEY and miR-205+PC3) have less DE genes than their counterparts that did induce it, which is expected since a morphological change is not observed. We expect that those treatments that induce MET would have more differentially expressed genes than those that do not, since a biological process is being induced within the cell. However, this trend does not hold true for the miR-429 overexpressed treatments. PC3 cells transfected with miR-429 showed 1,447 DE genes, while HEY transfected with the same microRNA showed 7,179 genes. It is unclear why PC3 cells have much fewer DE genes than HEY when both are transfected with miR-429. To elucidate why this may be the case, we compared the number of putative direct microRNA targets to our DE gene results, which revealed that 27% of PC3+miR-429's DE genes are direct putative targets of miR-429 (Figure 4). Comparing this to HEY+miR-429's DE genes, which had only 19% as putative direct targets of miR-429, this suggests that miR-429 induces MET in PC3 cells in a more direct

manner than it does in HEY. It may be that miR-429's induction of MET in HEY is driven more by the indirect effects of the microRNA, and in PC3 cells MET is induced primarily through the direct targets of miR-429. Further studies focused on the intersection of the differentially expressed genes in these two cell lines transfected with miR-429 may reveal genes common to both that induce a full MET process in PC3 and at least a partial induction of MET in HEY cells. Regarding the putative direct targets' relationship with the DE genes of other treatments that did or did not induce MET, there is not a clear relationship that demonstrates that the treatments that showed MET had a higher percentage of putative direct microRNA targets, and vice versa for those that did not demonstrate MET.

Another goal of this study was to identify a gene target for siRNA knockdown which may help elucidate a mechanism by which miR-429, miR-203a, and miR-205 induce MET in the cell lines. Based on aggregating the most common DE genes of all four samples that induced MET (HEY + miR-429, PC3 + miR-429, HEY + miR-205, and PC3 + miR-203a), which gave a list of 312 genes (figure 5), and then comparing these genes to Qiagen's list of EMT genes, four genes were identified as preliminary gene targets of interest: GNG11, TCF4, WNT5A, and ZEB1. Of these four, ZEB1 was identified as the primary siRNA knockdown candidate because it was a target of all three microRNAs of interest in this study, as well as due to its extensive involvement in EMT and many pathways involved in EMT [26].

The four genes are all implicated in EMT processes. GNG11, as classified by Qiagen's EMT list, is involved in G-protein coupled receptors in signaling pathways and normally upregulated during EMT. TCF4 is a transcription factor that binds with β-catenin to the promoter region of ZEB1 to induce its expression, and is normally upregulated during EMT [24].

WNT5A is involved in differentiation and development and upregulated during EMT, per Qiagen's list. It is also reported that WNT5A is involved in the regulation of cancer cell invasion, metastasis, metabolism, and inflammation [25]. Finally, ZEB1, per Qiagen's list, is involved in cell growth and proliferation, and is a transcription factor involved in EMT. It well-covered in the literature that ZEB1 is regulated by multiple signaling pathways, including WNT, NF-kB, TGF-β, and with the miR-200 family and miR-205 [26]. ZEB1's role of binding to the promoter of CDH1, the gene encoding E-cadherin, and repressing the expression of E-cadherin, thereby inducing EMT, is also well-reported [26]. ZEB1 acts in a double negative feedback loop with the miR-200 family to induce EMT when the miR-200 family is repressed [28]. It has also been shown to inhibit the expression of stemness-repressing microRNAs, including miR-203 and the miR-200 family, thereby increasing the tumorigenicity of pancreatic cancer cells [27]. ZEB1's role in EMT/MET is well-reported, and as such, it serves as a promising siRNA knockdown candidate to recapitulate MET. However, due to the inter-relatedness of genes involved in metastasis and EMT/MET, it is possible that ZEB1 knockdown may fail to recapitulate MET to the degree with which it was observed with the microRNAs. In this case, it is likely that the induction of MET with microRNAs is driven more so by the indirect effects of the microRNAs rather than its direct targets. This would be confirmed by siRNA knockdown of ZEB1 and resulting microarray analysis.

In order to understand how the microRNAs induced changes in gene expression, pathway enrichment of each treatment sample was done. For the miR-429 treatments, there were no common pathways enriched for HEY and PC3 cells. PC3+miR-429 pathway enrichments revealed enrichment for pathways such as cell junction organization, adherens junctions

interactions, and extracellular matrix organization, which are involved in cell adhesion changes affected by MET (ST4, Appendix). By contrast, the top enrichments for HEY+miR-429 are mostly involved in mitochondrial translation, gene expression, and cell cycle control. Because miR-429 induces MET in both HEY and PC3, these different enrichments suggest that miR-429 induces MET by different pathways in each cell line. The two other treatments that induced MET, PC3+miR-203a and HEY+miR-205, shared 131 pathways. This suggests there is some similarity in how MET is induced by these two microRNAs in HEY and PC3 cells, and these 131 pathways are each about 50% of the pathways enriched in these two treatments. Of note, inhibition of the mTOR signaling pathway, which is enriched in HEY+miR-205, PC3+ miR-203a, and the 312 MET gene list has been shown to cancel TGF-beta1 induced EMT in cervical cancer cells [23]. For the miR-205 treatments, there were 124 shared pathways, and although miR-205 did not induce MET in both cell lines, this suggests that miR-205 works through the many of the same pathways in both cell lines, but there are more indirect effects at play to induce MET in HEY cells. For the miR-203a treatments, there was only one shared pathway, extracellular matrix organization. This single shared pathway in two treatments that do not both show MET when using the same microRNA suggests that miR-203a induced MET in PC3 cells through a completely separate pathway than through which it may have acted on HEY cells.

All treatments showed enrichment in at least one of the pathways known to be involved in EMT/MET (highlighted in red on ST8), such as cell cycle, mitotic G2-G2/M phases, extracellular matrix organization, and mCalpain and friends in cell motility, among many others. The cellular stress response pathway was also enriched, which is due to the stress of transfection with Lipofectamine 2000. The six treatments that showed MET after

overexpression of one of the microRNAs were not all enriched in the same pathway at once, but there were different combinations of common enrichment (ST8, Appendix). Examples of such combinations include cell cycle and hedgehog 'on' state pathway enrichment which were enriched in HEY+429, HEY+205, PC3+203a, and PC3+205 (ST8, Appendix). Cell cycle arrest is common in EMT induction, many times arresting the cell at the G2 checkpoint [21]. Activation of the hedgehog pathway has been reported to indirectly induce EMT through FGF, Notch, TGF-beta signaling cascades, and microRNA regulatory networks [22]. These pathways have been shown to be induced in EMT, but PC3+miR-205 was not one of the MET-inducing treatments, which suggests that there are other pathways significant to prevent MET from occurring in PC3 cells when miR-205 is overexpressed. Not all pathways enriched are necessarily implicated in EMT/MET, as many of the enrichment results are quite general, such as 'gene expression.' Our study shows a more global understanding of the relationships between how microRNAs behave in similar cell lines.

CONCLUSION

In this study we provide many observations on how different microRNAs that have been shown to be involved in epithelial-to-mesenchymal transition successfully or unsuccessfully induce MET in two mesenchymal-like cell lines representative of ovarian and prostate cancer. Future work can further elucidate specific mechanisms of MET/EMT in different cell lines, beginning with the knockdown of ZEB1 as this study reveals it as a promising candidate to recapitulate MET. However, it is possible that the single-gene nature of using siRNA knockdown

of ZEB1 will be insufficient to recapitulate the complex process of MET. In this case, different combinations of gene targets may be used to attempt to recapitulate MET. However, if ZEB1 successfully recapitulates MET further studies may determine delivery methods of ZEB1 that can make it a useful therapeutic. Further work may also include studying these microRNAs in additional ovarian and prostate cancer cell lines to continue to pinpoint mechanisms that are similar in the induction of MET.

REFERENCES

[1] Jemal A, Siegel R, Ward E, Hao Y, Xu J, Murray T, Thun MJ. 2008. Cancer statistics, 2008. CA: a cancer journal for clinicians. 58(2):71-96.

[2] Iwatsuki M, Mimori K, Yokobori T, Ishi H, Beppu T, Nakamori S, Baba H, Mori M. 2010. Epithelial-mesenchymal transition in cancer development and its clinical significance. Cancer science. 101(2):293-299.

[3] Brabletz T. 2012. To differentiate or not--routes towards metastasis. Nature reviews Cancer. 12(6):425-436.

[4] Garofalo M, Croce CM. 2011. MicroRNAs: Master regulators as potential therapeutics in cancer. In: Cho AK, editor. Annual review of pharmacology and toxicology, vol 51, 2011. Palo Alto: Annual Reviews. p. 25-43.

[5] Chen J, Wang LJ, Matyunina LV, Hill CG, McDonald JF. 2011. Overexpression of mir-429 induces mesenchymal-to epithelial transition (MET) in metastatic ovarian cancer cells. Gynecologic Oncology. 121(1):200-205.

[6] Viticchie G, Lena AM, Latina A, Formosa A, Gregersen LH, Lund AH, Bernardini S, Mauriello A, Miano R, Spagnoli LG et al. 2011. Mir-203 controls proliferation, migration and invasive potential of prostate cancer cell lines. Cell Cycle. 10(7):1121-1131.

[7] Wang N, Li Q, Feng N-H, Cheng G, Guan Z-L, Wang Y, Qin C, Yin C-J, Hua L-X. 2013. Mir-205 is frequently downregulated in prostate cancer and acts as a tumor suppressor by inhibiting tumor growth. Asian Journal of Andrology. 15(6):735-741.

[8] Zhang M, Matyunina LV, Walker LD, Chen W, Xiao H, Benigno BB, Wu R, McDonald JF. 2017. Evidence for the importance of post-transcriptional regulatory changes in ovarian cancer progression and the contribution of mirnas. Sci Rep. 7(1):8171.

[9] Sossey-Alaoui K, Bialkowska K, Plow EF. 2009. The miR-200 family of microRNAs regulates wave3-dependent cancer cell invasion. Journal of Biological Chemistry. 284(48):33019-33029.

[10] Lili LN, Matyunina LV, Walker LD, Daneker GW, McDonald JF. 2014. Evidence for the importance of personalized molecular profiling in pancreatic cancer. Pancreas. 43(2):198-211.

[11] Lee CG, McCarthy S, Gruidl M, Timme C, Yeatman TJ. 2014. MicroRNA-147 Induces a Mesenchymal-To-Epithelial Transition (MET) and Reverses EGFR Inhibitor Resistance. PLOS ONE. 9(1):e84597.

[12] Betel D, Wilson M, Gabow A, Marks DS, Sander C. 2008. The microrna.Org resource: Targets and expression. Nucleic Acids Research. 36(Database issue):D149-D153.

[13] National Center for Health Statistics. Health, United States, 2016: With Chartbook on Long-term Trends in Health. Hyattsville, MD.

[14] Budczies J, von Winterfeld M, Klauschen F, Bockmayr M, Lennerz JK, Denkert C, Wolf T, Warth A, Dietel M, Anagnostopoulos I et al. 2015. The landscape of metastatic progression patterns across major human cancers. Oncotarget. 6(1):570-583.

[15] Halkia E, Spiliotis J, Sugarbaker P. 2012. Diagnosis and management of peritoneal metastases from ovarian cancer. Gastroenterol Res Pract. 2012:541842.

[16] Fang D, Chen H, Zhu JY, Wang W, Teng Y, Ding H-F, Jing Q, Su S-B, Huang S. 2017. Epithelial-mesenchymal transition of ovarian cancer cells is sustained by rac1 through simultaneous activation of mek1/2 and src signaling pathways. Oncogene. 36(11):1546-1558.

[17] Lo UG, Lee C-F, Lee M-S, Hsieh J-T. 2017. The role and mechanism of epithelial-to-mesenchymal transition in prostate cancer progression. International Journal of Molecular Sciences. 18(10):2079.

[18] Peng Y, Croce CM. 2016. The role of MicroRNAs in human cancer. Signal Transduction And Targeted Therapy. 1:15004.

[19] Zaravinos A. 2015. The regulatory role of microRNAs in EMT and cancer. Journal of Oncology. 2015:13.

[20] 2014. EMT gene list for RT² Profiler™ PCR Array Human Epithelial to Mesenchymal Transition (EMT) (PAHS-090Z). Qiagen. https://www.qiagen.com/us/shop/pcr/primer-sets/rt2-profiler-pcr-arrays/?catno=PAHS-090Z#geneglobe.

[21] Vega S, Morales AV, Ocaña OH, Valdés F, Fabregat I, Nieto MA. 2004. Snail blocks the cell cycle and confers resistance to cell death. Genes & Development. 18(10):1131-1143.

[22] Katoh Y, Katoh M. 2008. Hedgehog signaling, epithelial-to-mesenchymal transition and miRNA (review). Int J Mol Med. 22(3):271-275.

[23] Cheng K-y, Hao M. 2017. Mammalian target of rapamycin (mTOR) regulates transforming growth factor-β(1) (TGF-β(1))-induced epithelial-mesenchymal transition via decreased pyruvate kinase m2 (PKM2) expression in cervical cancer cells. Medical Science Monitor: International Medical Journal of Experimental and Clinical Research. 23:2017-2028.

[24] Sanchez-Tillo E, de Barrios O, Siles L, Cuatrecasas M, Castells A, Postigo A. 2011. Beta-catenin/TCF4 complex induces the epithelial-to-mesenchymal transition (EMT)-activator ZEB11 to regulate tumor invasiveness. Proc Natl Acad Sci U S A. 108(48):19204-19209.

[25] Asem MS, Buechler S, Wates RB, Miller DL, Stack MS. 2016. Wnt5a signaling in cancer. Cancers. 8(9):79.

[26] Zhang P, Sun Y, Ma L. 2015. Zeb1: At the crossroads of epithelial-mesenchymal transition, metastasis and therapy resistance. Cell Cycle. 14(4):481-487.

[27] Wellner U, Schubert J, Burk UC, Schmalhofer O, Zhu F, Sonntag A, Waldvogel B, Vannier C, Darling D, zur Hausen A et al. 2009. The emt-activator zeb1 promotes tumorigenicity by repressing stemness-inhibiting micrornas. Nat Cell Biol. 11(12):1487-1495.

[28] Gregory PA, Bert AG, Paterson EL, Barry SC, Tsykin A, Farshid G, Vadas MA, Khew-Goodall Y, Goodall GJ. 2008. The mir-200 family and mir-205 regulate epithelial to mesenchymal transition by targeting zeb1 and sip1. Nature Cell Biology. 10:593.

APPENDIX

Supplementary Tables (ST)

ST 1. HEY + miR-429 pathway enrichment results – top 50 pathway enrichments of 160 (ToppGene, FDR: $p < 0.05$)

Name	Source	p-value
Gene Expression	BioSystems: REACTOME	9.42E-18
Organelle biogenesis and maintenance	BioSystems: REACTOME	4.56E-12
Mitochondrial translation initiation	BioSystems: REACTOME	1.27E-10
Mitochondrial translation elongation	BioSystems: REACTOME	2.37E-10
Mitochondrial translation	BioSystems: REACTOME	5.78E-10
Mitochondrial translation termination	BioSystems: REACTOME	1.91E-09
Cell Cycle	BioSystems: REACTOME	2.78E-09
Generic Transcription Pathway	BioSystems: REACTOME	5.20E-09
Metabolism of proteins	BioSystems: REACTOME	5.69E-09
Cell Cycle, Mitotic	BioSystems: REACTOME	3.91E-08
Respiratory electron transport, ATP synthesis by chemiosmotic coupling, and heat production by uncoupling proteins.	BioSystems: REACTOME	5.55E-08
Respiratory electron transport	BioSystems: REACTOME	1.07E-07
Mitotic G2-G2/M phases	BioSystems: REACTOME	1.87E-07
G2/M Transition	BioSystems: REACTOME	2.27E-07
The citric acid (TCA) cycle and respiratory electron transport	BioSystems: REACTOME	2.38E-07
Post-translational protein modification	BioSystems: REACTOME	6.18E-07
Validated targets of C-MYC transcriptional activation	BioSystems: Pathway Interaction Database	8.31E-07
Cellular responses to stress	BioSystems: REACTOME	9.61E-07
S Phase	BioSystems: REACTOME	1.29E-06
Lysine degradation	BioSystems: KEGG	1.76E-06
Oxidative phosphorylation	BioSystems: KEGG	1.80E-06
The role of GTSE1 in G2/M progression after G2 checkpoint	BioSystems: REACTOME	4.27E-06
Non-alcoholic fatty liver disease (NAFLD)	BioSystems: KEGG	4.45E-06
Regulation of ornithine decarboxylase (ODC)	BioSystems: REACTOME	5.03E-06
Synthesis of DNA	BioSystems: REACTOME	5.78E-06
APC/C:Cdh1 mediated degradation of Cdc20 and other APC/C:Cdh1 targeted proteins in late mitosis/early G1	BioSystems: REACTOME	1.27E-05
Cyclin A:Cdk2-associated events at S phase entry	BioSystems: REACTOME	1.55E-05
TP53 Regulates Metabolic Genes	BioSystems: REACTOME	1.93E-05

oxidative phosphorylation	Pathway Ontology	2.07E-05
Cyclin E associated events during G1/S transition	BioSystems: REACTOME	2.34E-05
Golgi Associated Vesicle Biogenesis	BioSystems: REACTOME	2.37E-05
Chromosome Maintenance	BioSystems: REACTOME	2.60E-05
Asparagine N-linked glycosylation	BioSystems: REACTOME	2.90E-05
Cilium Assembly	BioSystems: REACTOME	3.22E-05
Antigen processing-Cross presentation	BioSystems: REACTOME	3.40E-05
APC/C:Cdc20 mediated degradation of Securin	BioSystems: REACTOME	3.46E-05
DNA Replication	BioSystems: REACTOME	3.57E-05
PCP/CE pathway	BioSystems: REACTOME	3.62E-05
SCF(Skp2)-mediated degradation of p27/p21	BioSystems: REACTOME	4.06E-05
Degradation of DVL	BioSystems: REACTOME	4.92E-05
Autodegradation of Cdh1 by Cdh1:APC/C	BioSystems: REACTOME	5.12E-05
Membrane Trafficking	BioSystems: REACTOME	5.46E-05
Ubiquitin-dependent degradation of Cyclin D	BioSystems: REACTOME	5.54E-05
Ubiquitin-dependent degradation of Cyclin D1	BioSystems: REACTOME	5.54E-05
Extension of Telomeres	BioSystems: REACTOME	5.58E-05
AUF1 (hnRNP D0) binds and destabilizes mRNA	BioSystems: REACTOME	5.97E-05
G1/S DNA Damage Checkpoints	BioSystems: REACTOME	6.32E-05
MAPK6/MAPK4 signaling	BioSystems: REACTOME	6.53E-05
Proteasome	BioSystems: KEGG	7.06E-05
p53-Dependent G1/S DNA damage checkpoint	BioSystems: REACTOME	7.70E-05

ST2. HEY + miR-203a pathway enrichment results - all pathway enrichments (ToppGene, FDR: $p < 0.05$)

Name	Source	p-value
Cytokine-cytokine receptor interaction	BioSystems: KEGG	1.30E-05
Starch and Sucrose Metabolism	SMPDB	2.23E-05
Digestion of dietary carbohydrate	BioSystems: REACTOME	3.26E-05
Extracellular matrix organization	BioSystems: REACTOME	3.66E-05
Starch and sucrose metabolism	BioSystems: KEGG	5.11E-05
Rheumatoid arthritis	BioSystems: KEGG	1.40E-04

ST3. HEY + miR-205 pathway enrichment results – top 50 of 255 pathway enrichments (ToppGene, FDR: $p < 0.05$)

Name	Source	p-value
Gene Expression	BioSystems: REACTOME	1.23E-17
Metabolism	BioSystems: REACTOME	1.95E-15
Metabolic pathways	BioSystems: KEGG	8.36E-15
Cell Cycle, Mitotic	BioSystems: REACTOME	1.16E-11
Cell Cycle	BioSystems: REACTOME	1.06E-10
Asparagine N-linked glycosylation	BioSystems: REACTOME	6.79E-10
Cellular responses to stress	BioSystems: REACTOME	7.83E-10

Organelle biogenesis and maintenance	BioSystems: REACTOME	2.04E-09
Metabolism of proteins	BioSystems: REACTOME	3.33E-09
Membrane Trafficking	BioSystems: REACTOME	8.15E-09
Class I MHC mediated antigen processing & presentation	BioSystems: REACTOME	8.84E-09
Post-translational protein modification	BioSystems: REACTOME	1.45E-07
Vesicle-mediated transport	BioSystems: REACTOME	1.47E-07
G2/M Transition	BioSystems: REACTOME	1.82E-07
Mitotic Metaphase and Anaphase	BioSystems: REACTOME	1.87E-07
Antigen processing: Ubiquitination & Proteasome degradation	BioSystems: REACTOME	2.26E-07
Mitotic Anaphase	BioSystems: REACTOME	2.80E-07
The citric acid (TCA) cycle and respiratory electron transport	BioSystems: REACTOME	3.14E-07
Mitotic G2-G2/M phases	BioSystems: REACTOME	3.85E-07
Mitochondrial translation initiation	BioSystems: REACTOME	4.26E-07
M Phase	BioSystems: REACTOME	1.04E-06
Separation of Sister Chromatids	BioSystems: REACTOME	2.19E-06
Mitochondrial translation	BioSystems: REACTOME	2.33E-06
Transcriptional Regulation by TP53	BioSystems: REACTOME	2.42E-06
PKB-mediated events	BioSystems: REACTOME	2.65E-06
TP53 Regulates Metabolic Genes	BioSystems: REACTOME	3.48E-06
S Phase	BioSystems: REACTOME	3.51E-06
Mitochondrial translation termination	BioSystems: REACTOME	3.57E-06
Metabolism of lipids and lipoproteins	BioSystems: REACTOME	3.97E-06
Biosynthesis of amino acids	BioSystems: KEGG	4.84E-06
mTOR signalling	BioSystems: REACTOME	5.13E-06
Mitochondrial translation elongation	BioSystems: REACTOME	5.95E-06
Regulation of mRNA stability by proteins that bind AU-rich elements	BioSystems: REACTOME	6.11E-06
Processing of Capped Intron-Containing Pre-mRNA	BioSystems: REACTOME	6.19E-06
Synthesis of DNA	BioSystems: REACTOME	6.26E-06
Parkinson's disease	BioSystems: KEGG	6.98E-06
COPII (Coat Protein 2) Mediated Vesicle Transport	BioSystems: REACTOME	7.45E-06
Beta-catenin independent WNT signaling	BioSystems: REACTOME	8.93E-06
Cyclin A:Cdk2-associated events at S phase entry	BioSystems: REACTOME	1.36E-05
Cdc20:Phospho-APC/C mediated degradation of Cyclin A	BioSystems: REACTOME	1.40E-05
Transport to the Golgi and subsequent modification	BioSystems: REACTOME	1.43E-05
Regulation of APC/C activators between G1/S and early anaphase	BioSystems: REACTOME	1.52E-05
Respiratory electron transport	BioSystems: REACTOME	1.53E-05
Signaling by Wnt	BioSystems: REACTOME	1.54E-05
ER to Golgi Anterograde Transport	BioSystems: REACTOME	1.68E-05
mRNA Splicing	BioSystems: REACTOME	2.02E-05
APC:Cdc20 mediated degradation of cell cycle proteins prior to satisfation of the cell cycle checkpoint	BioSystems: REACTOME	2.35E-05

Biosynthesis of the N-glycan precursor (dolichol lipid-linked oligosaccharide, LLO) and transfer to a nascent protein	BioSystems: REACTOME	2.39E-05
RNA transport	BioSystems: KEGG	2.50E-05
Energy dependent regulation of mTOR by LKB1-AMPK	BioSystems: REACTOME	2.80E-05

ST4. PC3 + miR-429 pathway enrichment results - all pathway enrichments (ToppGene, FDR: $p < 0.05$)

Name	Source	p-value
Cell junction organization	BioSystems: REACTOME	6.58E-07
Proteoglycans in cancer	BioSystems: KEGG	6.84E-07
Cell-cell junction organization	BioSystems: REACTOME	1.22E-06
Hippo signaling pathway	BioSystems: KEGG	5.07E-06
Pathways in cancer	BioSystems: KEGG	6.50E-06
Cell-Cell communication	BioSystems: REACTOME	1.33E-05
Adherens junctions interactions	BioSystems: REACTOME	1.46E-05
Fluid shear stress and atherosclerosis	BioSystems: KEGG	3.49E-05
Glycosaminoglycan metabolism	BioSystems: REACTOME	4.35E-05
Signaling by MST1	BioSystems: REACTOME	8.04E-05
mucin core 1 and core 2 O-glycosylation	BioSystems: BIOCYC	1.14E-04
Amoebiasis	BioSystems: KEGG	1.17E-04
Extracellular matrix organization	BioSystems: REACTOME	1.85E-04

ST5. PC3 + miR-203a pathway enrichment results – top 50 of 261 pathway enrichments (ToppGene, FDR: $p < 0.05$)

Name	Source	p-value
Gene Expression	BioSystems: REACTOME	1.42E-20
Metabolism of proteins	BioSystems: REACTOME	3.66E-15
Metabolism	BioSystems: REACTOME	2.54E-12
rRNA processing in the nucleus and cytosol	BioSystems: REACTOME	2.00E-11
Organelle biogenesis and maintenance	BioSystems: REACTOME	3.90E-11
rRNA processing	BioSystems: REACTOME	5.53E-11
Infectious disease	BioSystems: REACTOME	1.08E-10
Cell Cycle, Mitotic	BioSystems: REACTOME	2.18E-10
Mitochondrial translation initiation	BioSystems: REACTOME	2.47E-10
Ribosome	BioSystems: KEGG	4.17E-10
Mitochondrial translation elongation	BioSystems: REACTOME	4.59E-10
Translation	BioSystems: REACTOME	6.98E-10
Major pathway of rRNA processing in the nucleolus and cytosol	BioSystems: REACTOME	1.09E-09
Mitochondrial translation	BioSystems: REACTOME	1.13E-09
Mitotic G2-G2/M phases	BioSystems: REACTOME	2.70E-09

Mitochondrial translation termination	BioSystems: REACTOME	3.56E-09
Eukaryotic Translation Elongation	BioSystems: REACTOME	5.74E-09
Metabolism of amino acids and derivatives	BioSystems: REACTOME	7.62E-09
G2/M Transition	BioSystems: REACTOME	7.90E-09
Cell Cycle	BioSystems: REACTOME	8.47E-09
Formation of a pool of free 40S subunits	BioSystems: REACTOME	1.55E-08
GTP hydrolysis and joining of the 60S ribosomal subunit	BioSystems: REACTOME	1.61E-08
L13a-mediated translational silencing of Ceruloplasmin expression	BioSystems: REACTOME	1.61E-08
Eukaryotic Translation Initiation	BioSystems: REACTOME	2.22E-08
Cap-dependent Translation Initiation	BioSystems: REACTOME	2.22E-08
SRP-dependent cotranslational protein targeting to membrane	BioSystems: REACTOME	3.56E-08
Eukaryotic Translation Termination	BioSystems: REACTOME	3.62E-08
Cellular responses to stress	BioSystems: REACTOME	5.06E-08
Peptide chain elongation	BioSystems: REACTOME	5.07E-08
Viral mRNA Translation	BioSystems: REACTOME	1.58E-07
Selenocysteine synthesis	BioSystems: REACTOME	2.10E-07
Metabolic pathways	BioSystems: KEGG	2.25E-07
Disease	BioSystems: REACTOME	2.46E-07
UCH proteinases	BioSystems: REACTOME	3.76E-07
Nonsense Mediated Decay (NMD) independent of the Exon Junction Complex (EJC)	BioSystems: REACTOME	4.25E-07
Membrane Trafficking	BioSystems: REACTOME	4.69E-07
Regulation of mRNA stability by proteins that bind AU-rich elements	BioSystems: REACTOME	4.70E-07
Antigen processing-Cross presentation	BioSystems: REACTOME	5.41E-07
ER-Phagosome pathway	BioSystems: REACTOME	7.99E-07
Influenza Infection	BioSystems: REACTOME	1.11E-06
Asparagine N-linked glycosylation	BioSystems: REACTOME	1.26E-06
Unfolded Protein Response (UPR)	BioSystems: REACTOME	1.34E-06
Influenza Viral RNA Transcription and Replication	BioSystems: REACTOME	1.35E-06
Selenoamino acid metabolism	BioSystems: REACTOME	1.48E-06
Influenza Life Cycle	BioSystems: REACTOME	2.04E-06
Vesicle-mediated transport	BioSystems: REACTOME	3.20E-06
HIV Infection	BioSystems: REACTOME	3.53E-06
Post-translational protein modification	BioSystems: REACTOME	4.85E-06
Metabolism of carbohydrates	BioSystems: REACTOME	4.86E-06
FBXL7 down-regulates AURKA during mitotic entry and in early mitosis	BioSystems: REACTOME	5.31E-06

ST6. PC3 + miR-205 pathway enrichment results – top 50 of 218 pathways enriched – (ToppGene, FDR: $p < 0.05$)

Name	Source	p-value

Interferon alpha/beta signaling	BioSystems: REACTOME	6.87E-13
Gene Expression	BioSystems: REACTOME	5.58E-11
Cell Cycle, Mitotic	BioSystems: REACTOME	7.31E-11
Metabolism	BioSystems: REACTOME	3.25E-10
Metabolism of proteins	BioSystems: REACTOME	1.72E-09
ER-Phagosome pathway	BioSystems: REACTOME	3.27E-09
Interferon Signaling	BioSystems: REACTOME	5.90E-09
Cell Cycle	BioSystems: REACTOME	6.13E-09
Protein processing in endoplasmic reticulum	BioSystems: KEGG	9.98E-09
Cytokine Signaling in Immune system	BioSystems: REACTOME	2.97E-08
Immune System	BioSystems: REACTOME	3.33E-08
Cellular responses to stress	BioSystems: REACTOME	3.90E-08
G2/M Transition	BioSystems: REACTOME	6.93E-08
M Phase	BioSystems: REACTOME	9.55E-08
Mitochondrial translation elongation	BioSystems: REACTOME	1.00E-07
Mitotic G2-G2/M phases	BioSystems: REACTOME	1.22E-07
Metabolism of amino acids and derivatives	BioSystems: REACTOME	1.36E-07
rRNA processing in the nucleus and cytosol	BioSystems: REACTOME	1.61E-07
Mitochondrial translation initiation	BioSystems: REACTOME	2.07E-07
rRNA processing	BioSystems: REACTOME	2.08E-07
Mitochondrial translation	BioSystems: REACTOME	3.99E-07
Unfolded Protein Response (UPR)	BioSystems: REACTOME	5.33E-07
Translation	BioSystems: REACTOME	6.01E-07
Mitochondrial translation termination	BioSystems: REACTOME	6.38E-07
Antigen processing-Cross presentation	BioSystems: REACTOME	1.01E-06
SCF(Skp2)-mediated degradation of p27/p21	BioSystems: REACTOME	1.26E-06
The role of GTSE1 in G2/M progression after G2 checkpoint	BioSystems: REACTOME	1.26E-06
Infectious disease	BioSystems: REACTOME	1.32E-06
Major pathway of rRNA processing in the nucleolus and cytosol	BioSystems: REACTOME	1.71E-06
Ribosome	BioSystems: KEGG	1.75E-06
Regulation of mRNA stability by proteins that bind AU-rich elements	BioSystems: REACTOME	4.27E-06
Organelle biogenesis and maintenance	BioSystems: REACTOME	4.27E-06
Cyclin E associated events during G1/S transition	BioSystems: REACTOME	4.89E-06
Biosynthesis of amino acids	BioSystems: KEGG	7.29E-06
IRE1alpha activates chaperones	BioSystems: REACTOME	7.72E-06
p53-Dependent G1/S DNA damage checkpoint	BioSystems: REACTOME	7.75E-06
p53-Dependent G1 DNA Damage Response	BioSystems: REACTOME	7.75E-06
Mitotic Metaphase and Anaphase	BioSystems: REACTOME	9.41E-06
Cyclin A:Cdk2-associated events at S phase entry	BioSystems: REACTOME	9.76E-06
XBP1(S) activates chaperone genes	BioSystems: REACTOME	1.03E-05
Hh mutants that don't undergo autocatalytic processing are degraded by ERAD	BioSystems: REACTOME	1.21E-05

Mitotic Anaphase	BioSystems: REACTOME	1.51E-05
Class I MHC mediated antigen processing & presentation	BioSystems: REACTOME	1.63E-05
G1/S DNA Damage Checkpoints	BioSystems: REACTOME	1.75E-05
Hedgehog ligand biogenesis	BioSystems: REACTOME	1.75E-05
Respiratory electron transport	BioSystems: REACTOME	1.76E-05
Eukaryotic Translation Initiation	BioSystems: REACTOME	1.95E-05
Cap-dependent Translation Initiation	BioSystems: REACTOME	1.95E-05
Membrane Trafficking	BioSystems: REACTOME	2.24E-05
Eukaryotic Translation Elongation	BioSystems: REACTOME	2.26E-05

ST7. 312 MET genes pathway enrichment results

Name	Source	p-value
IL23-mediated signaling events	BioSystems: Pathway Interaction Database	1.37E-03
PI3K-Akt signaling pathway	BioSystems: KEGG	1.90E-03
Histidine, lysine, phenylalanine, tyrosine, proline and tryptophan catabolism	BioSystems: REACTOME	2.84E-03
Hypoxia and p53 in the Cardiovascular system	MSigDB C2 BIOCARTA (v6.0)	3.28E-03
mTOR signaling pathway	BioSystems: KEGG	3.83E-03
mCalpain and friends in Cell motility	MSigDB C2 BIOCARTA (v6.0)	4.17E-03
Toll receptor signaling pathway	PantherDB	4.17E-03
ECM-receptor interaction	BioSystems: KEGG	4.50E-03
Synthesis of diphthamide-EEF2	BioSystems: REACTOME	4.58E-03
CHL1 interactions	BioSystems: REACTOME	5.84E-03
Longevity regulating pathway	BioSystems: KEGG	6.37E-03
Ca-dependent events	BioSystems: REACTOME	7.02E-03
Collagen formation	BioSystems: REACTOME	7.65E-03
Amoebiasis	BioSystems: KEGG	8.71E-03
IRAK4 deficiency (TLR2/4)	BioSystems: REACTOME	8.77E-03
MyD88 deficiency (TLR2/4)	BioSystems: REACTOME	8.77E-03
Inflammatory mediator regulation of TRP channels	BioSystems: KEGG	9.09E-03
Glucagon signaling in metabolic regulation	BioSystems: REACTOME	9.17E-03
AKAP95 role in mitosis and chromosome dynamics	MSigDB C2 BIOCARTA (v6.0)	1.04E-02
Cystic Fibrosis Transmembrane Conductance Regulator And Beta 2 Adrenergic Receptor Pathway	MSigDB C2 BIOCARTA (v6.0)	1.04E-02
IL1-mediated signaling events	BioSystems: Pathway Interaction Database	1.08E-02
Prion diseases	BioSystems: KEGG	1.08E-02
Signaling events mediated by TCPTP	BioSystems: Pathway Interaction Database	1.17E-02
GABA-B receptor II signaling	PantherDB	1.17E-02
Toll-like receptor signaling pathway	BioSystems: KEGG	1.21E-02
Aspartate Metabolism	SMPDB	1.22E-02
Notch-HLH transcription pathway	BioSystems: REACTOME	1.22E-02

Platelet Adhesion to exposed collagen	BioSystems: REACTOME	1.22E-02
Argininosuccinic Aciduria	SMPDB	1.34E-02
oxidative stress responses	Pathway Ontology	1.34E-02
Methylmalonate Semialdehyde Dehydrogenase Deficiency	SMPDB	1.34E-02
Interleukin-6 signaling	Pathway Ontology	1.34E-02
Signaling events mediated by HDAC Class III	BioSystems: Pathway Interaction Database	1.45E-02
Endothelin signaling pathway	PantherDB	1.56E-02
Inositol Metabolism	SMPDB	1.62E-02
Protein Kinase A at the Centrosome	MSigDB C2 BIOCARTA (v6.0)	1.62E-02
Glycosphingolipid biosynthesis - globo and isoglobo series	BioSystems: KEGG	1.62E-02
The IGF-1 Receptor and Longevity	MSigDB C2 BIOCARTA (v6.0)	1.62E-02
Cholinergic synapse	BioSystems: KEGG	1.62E-02
Focal adhesion	BioSystems: KEGG	1.63E-02
Gastric acid secretion	BioSystems: KEGG	1.71E-02
Extracellular matrix organization	BioSystems: REACTOME	1.72E-02
Glucagon-like Peptide-1 (GLP1) regulates insulin secretion	BioSystems: REACTOME	1.77E-02
Pertussis	BioSystems: KEGG	1.79E-02
Proteoglycans in cancer	BioSystems: KEGG	1.80E-02
Role of PI3K subunit p85 in regulation of Actin Organization and Cell Migration	MSigDB C2 BIOCARTA (v6.0)	1.83E-02
Regulation of TLR by endogenous ligand	BioSystems: REACTOME	1.83E-02
PKA activation	BioSystems: REACTOME	1.83E-02
B Cell Survival Pathway	MSigDB C2 BIOCARTA (v6.0)	1.83E-02
Vasopressin regulates renal water homeostasis via Aquaporins	BioSystems: REACTOME	1.88E-02

ST8. Summary of common pathway enrichment among miRNA treatments of HEY and PC3 cells (1 = pathway enriched, red text = pathways shown to be involved in EMT)

ID	Name	H_429	H_203a	H_205	P_429	P_203a	P_205	312_MET
1269649	Gene Expression	1		1		1	1	
1268838	Organelle biogenesis and maintenance	1		1		1	1	
1268843	Mitochondrial translation initiation	1		1		1	1	
1268844	Mitochondrial translation elongation	1		1		1	1	
1268842	Mitochondrial translation	1		1		1	1	
1268845	Mitochondrial translation termination	1		1		1	1	
1269741	Cell Cycle	1		1		1	1	

1269650	Generic Transcription Pathway	1		1		1		
1268677	Metabolism of proteins	1		1		1	1	
1269763	Cell Cycle, Mitotic	1		1		1	1	
1270127	Respiratory electron transport, ATP synthesis by chemiosmotic coupling, and heat production by uncoupling proteins.	1		1		1	1	
1270128	Respiratory electron transport	1		1		1	1	
1269797	Mitotic G2-G2/M phases	1		1		1	1	
1269799	G2/M Transition	1		1		1	1	
1270121	The citric acid (TCA) cycle and respiratory electron transport	1		1		1	1	
1268701	Post-translational protein modification	1		1		1	1	
169351	Validated targets of C-MYC transcriptional activation	1		1		1		
1270414	Cellular responses to stress	1		1		1	1	
1269777	S Phase	1		1		1	1	
82942	Oxidative phosphorylation	1		1		1		
1383017	The role of GTSE1 in G2/M progression after G2 checkpoint	1		1		1	1	
862188	Non-alcoholic fatty liver disease (NAFLD)	1		1		1		
1270174	Regulation of ornithine decarboxylase (ODC)	1		1		1	1	
1269779	Synthesis of DNA	1		1		1	1	
1269851	APC/C:Cdh1 mediated degradation of Cdc20 and other APC/C:Cdh1	1		1		1	1	

	targeted proteins in late mitosis/early G1							
1269778	Cyclin A:Cdk2-associated events at S phase entry	1		1		1	1	
1269655	TP53 Regulates Metabolic Genes	1		1			1	
PW:0000034	oxidative phosphorylation	1		1		1		
1269769	Cyclin E associated events during G1/S transition	1		1		1	1	
1269882	Golgi Associated Vesicle Biogenesis	1		1				
1269853	Chromosome Maintenance	1		1		1		
1268714	Asparagine N-linked glycosylation	1		1		1	1	
1268846	Cilium Assembly	1		1		1		
1269195	Antigen processing-Cross presentation	1				1	1	
1269849	APC/C:Cdc20 mediated degradation of Securin	1		1		1	1	
1269875	DNA Replication	1		1		1	1	
1269611	PCP/CE pathway	1		1		1	1	
1269770	SCF(Skp2)-mediated degradation of p27/p21	1		1		1	1	
1269605	Degradation of DVL	1				1	1	
1269852	Autodegradation of Cdh1 by Cdh1:APC/C	1		1		1	1	
1269877	Membrane Trafficking	1		1		1	1	
1269791	Ubiquitin-dependent degradation of Cyclin D	1		1		1	1	
1269792	Ubiquitin-dependent degradation of Cyclin D1	1		1		1	1	
1269857	Extension of Telomeres	1		1				

1269726	AUF1 (hnRNP D0) binds and destabilizes mRNA	1		1		1	1	
1269743	G1/S DNA Damage Checkpoints	1		1		1	1	
1269506	MAPK6/MAPK4 signaling	1		1		1	1	
83040	Proteasome	1				1	1	
1269744	p53-Dependent G1/S DNA damage checkpoint	1		1		1	1	
1269745	p53-Dependent G1 DNA Damage Response	1		1		1	1	
1427860	Deubiquitination	1		1		1	1	
1269725	Regulation of mRNA stability by proteins that bind AU-rich elements	1		1		1	1	
1383018	AURKA Activation by TPX2	1		1		1	1	
1270296	Regulation of activated PAK-2p34 by proteasome mediated degradation	1		1		1	1	
1269881	Clathrin derived vesicle budding	1		1				
1269880	trans-Golgi Network Vesicle Budding	1		1				
1457807	FBXL7 down-regulates AURKA during mitotic entry and in early mitosis	1				1	1	
1427861	UCH proteinases	1		1		1	1	
1269845	APC:Cdc20 mediated degradation of cell cycle proteins prior to satisfation of the cell cycle checkpoint	1		1		1	1	
1270170	Metabolism of polyamines	1		1		1	1	
1269640	Hedgehog 'on' state	1		1		1	1	
1270295	Regulation of Apoptosis	1		1		1	1	
132956	Metabolic pathways	1		1		1	1	

177876	RNA transport	1		1				
1269842	Activation of APC/C and APC/C:Cdc20 mediated degradation of mitotic proteins	1		1		1	1	
1268847	Anchoring of the basal body to the plasma membrane	1		1		1	1	
1269197	ER-Phagosome pathway	1				1	1	
1269612	Asymmetric localization of PCP proteins	1		1		1	1	
1268934	Defective CFTR causes cystic fibrosis	1				1	1	
1269808	Loss of proteins required for interphase microtubule organization from the centrosome	1		1		1	1	
1269809	Loss of Nlp from mitotic centrosomes	1		1		1	1	
1269098	Vif-mediated degradation of APOBEC3G	1				1	1	
1269876	Vesicle-mediated transport	1		1		1	1	
1269654	Transcriptional Regulation by TP53	1		1		1	1	
1269742	Cell Cycle Checkpoints	1		1		1	1	
1269846	Cdc20:Phospho-APC/C mediated degradation of Cyclin A	1		1		1	1	
125136	Spliceosome	1		1		1	1	
1269747	Autodegradation of the E3 ubiquitin ligase COP1	1				1	1	
1268928	Hh mutants that don't undergo autocatalytic processing are degraded by ERAD	1		1		1	1	

1269844	APC/C:Cdc20 mediated degradation of mitotic proteins	1		1		1	1	
1269199	Cross-presentation of soluble exogenous antigens (endosomes)	1				1	1	
1269746	Stabilization of p53	1				1	1	
1269751	p53-Independent DNA Damage Response	1				1	1	
1269750	p53-Independent G1/S DNA damage checkpoint	1				1	1	
1269752	Ubiquitin Mediated Degradation of Phosphorylated Cdc25A	1				1	1	
1269806	Recruitment of mitotic centrosome proteins and complexes	1		1		1	1	
1269805	Centrosome maturation	1		1		1	1	
1269784	DNA strand elongation	1		1				
1270418	Oxygen-dependent proline hydroxylation of Hypoxia-inducible Factor Alpha	1				1		
83098	Parkinson's disease	1		1		1	1	
1427862	Ub-specific processing proteases	1					1	
1269783	CDK-mediated phosphorylation and removal of Cdc6	1				1	1	
1269610	Beta-catenin independent WNT signaling	1		1		1	1	
1269810	M Phase	1		1		1	1	
1270262	Apoptosis	1		1			1	
1270125	Citric acid cycle (TCA cycle)	1		1				
1270261	Programmed Cell Death	1		1			1	

1268927	Hh mutants abrogate ligand secretion	1				1	1	
1339146	Complex I biogenesis	1		1		1	1	
1269768	G1/S Transition	1		1		1	1	
373901	HTLV-I infection	1						1
1269825	Mitotic Anaphase	1		1		1	1	
1269599	TCF dependent signaling in response to WNT	1		1		1	1	
1269290	Regulation of RAS by GAPs	1		1		1	1	
1269838	APC/C-mediated degradation of cell cycle proteins	1		1			1	
1269837	Regulation of mitotic cell cycle	1		1			1	
1269107	Vpu mediated degradation of CD4	1				1	1	
469200	Legionellosis	1					1	1
1269304	CLEC7A (Dectin-1) signaling	1		1		1	1	
1269637	GLI3 is processed to GLI3R by the proteasome	1		1		1	1	
1269823	Mitotic Metaphase and Anaphase	1		1		1	1	
1269841	SCF-beta-TrCP mediated degradation of Emi1	1		1		1	1	
1269764	Mitotic G1-G1/S phases	1		1		1	1	
83097	Alzheimer's disease	1		1				
1269781	Switching of origins to a post-replicative state	1		1		1	1	
1269782	Orc1 removal from chromatin	1		1		1	1	
1269956	Metabolism	1		1		1	1	
1269594	Signaling by Wnt	1		1		1	1	
1270350	DNA Repair	1		1		1		
1269856	Telomere Maintenance	1				1		
1269839	Regulation of APC/C activators between	1		1			1	

	G1/S and early anaphase							
1269826	Separation of Sister Chromatids	1		1		1	1	
1269331	NIK-->noncanonical NF-kB signaling	1		1		1	1	
1268725	Transport to the Golgi and subsequent modification	1		1		1		
1268726	ER to Golgi Anterograde Transport	1		1				
1269796	Removal of licensing factors from origins	1		1		1	1	
1269688	Processing of Capped Intron-Containing Pre-mRNA	1		1		1	1	
1269794	Regulation of DNA replication	1				1	1	
1269306	Dectin-1 mediated noncanonical NF-kB signaling	1		1		1	1	
1269638	Degradation of GLI2 by the proteasome	1				1	1	
1269833	Assembly of the pre-replicative complex	1				1	1	
1268933	ABC transporter disorders	1				1	1	
1270367	DNA Damage Bypass	1					1	
1269803	Regulation of PLK1 Activity at G2/M Transition	1				1	1	
1269606	Degradation of AXIN	1		1		1	1	
1269689	mRNA Splicing	1		1		1	1	
1269831	M/G1 Transition	1				1	1	
1269832	DNA Replication Pre-Initiation	1				1	1	
1269634	Hedgehog ligand biogenesis	1				1	1	
1270244	Extracellular matrix organization		1		1	1		1
200309	Rheumatoid arthritis		1					1
1268760	XBP1(S) activates chaperone genes			1		1	1	

83100	Huntington's disease			1		1		
1269690	mRNA Splicing - Major Pathway			1		1		
1269957	Metabolism of carbohydrates			1		1		
1269596	Degradation of beta-catenin by the destruction complex			1		1	1	
1270158	Metabolism of amino acids and derivatives			1		1	1	
1457780	Neutrophil degranulation			1		1	1	
1269056	Infectious disease			1		1	1	
1269171	Adaptive Immune System			1			1	
814926	Carbon metabolism			1		1	1	
1269057	HIV Infection			1		1	1	
1269639	Degradation of GLI1 by the proteasome			1		1	1	
M8719	mCalpain and friends in Cell motility			1				1
1269194	Antigen Presentation: Folding, assembly and peptide loading of class I MHC			1			1	
1269170	Immune System			1		1	1	
1270426	Cellular Senescence			1		1	1	
1269821	Resolution of Sister Chromatid Cohesion			1			1	
1383038	Intra-Golgi and retrograde Golgi-to-ER traffic			1		1	1	
138001	mTOR signaling pathway			1		1		
SMP00011	Inositol Metabolism			1				1
658418	Viral carcinogenesis			1		1	1	1
1383086	Major pathway of rRNA processing in the nucleolus and cytosol			1		1	1	
1319989	Longevity regulating pathway			1				1

1269186	Activation of NF-kappaB in B cells			1		1	1	
1427846	rRNA processing in the nucleus and cytosol			1		1	1	
1383042	COPI-dependent Golgi-to-ER retrograde traffic			1		1	1	
1269959	Glucose metabolism			1		1	1	
1269883	Lysosome Vesicle Biogenesis			1		1		
1383085	rRNA processing			1		1	1	
1269734	Epigenetic regulation of gene expression			1		1		
M8873	Fas Signaling Pathway			1		1		
1269633	Signaling by Hedgehog			1		1	1	
1383087	rRNA modification in the nucleus and cytosol			1		1	1	
M16563	mTOR Signaling Pathway			1		1		1
782000	Proteoglycans in cancer				1			1
83105	Pathways in cancer				1			1
1474302	Fluid shear stress and atherosclerosis				1	1	1	
167324	Amoebiasis				1			1
83036	Ribosome					1	1	
1268678	Translation					1	1	
1268690	Eukaryotic Translation Elongation					1	1	
1268681	Formation of a pool of free 40S subunits					1	1	
1268686	GTP hydrolysis and joining of the 60S ribosomal subunit					1	1	
1268688	L13a-mediated translational silencing of Ceruloplasmin expression					1	1	

1268679	Eukaryotic Translation Initiation					1	1	
1268680	Cap-dependent Translation Initiation					1	1	
1268689	SRP-dependent cotranslational protein targeting to membrane					1	1	
1268692	Eukaryotic Translation Termination					1	1	
1268691	Peptide chain elongation					1	1	
1269120	Viral mRNA Translation					1	1	
1339156	Selenocysteine synthesis					1	1	
1268854	Disease					1	1	
1269718	Nonsense Mediated Decay (NMD) independent of the Exon Junction Complex (EJC)					1	1	
1269108	Influenza Infection					1	1	
1268756	Unfolded Protein Response (UPR)					1	1	
1269115	Influenza Viral RNA Transcription and Replication					1	1	
1339149	Selenoamino acid metabolism					1	1	
1269109	Influenza Life Cycle					1	1	
1268759	IRE1alpha activates chaperones					1	1	
1269717	Nonsense Mediated Decay (NMD) enhanced by the Exon Junction Complex (EJC)					1	1	
1269716	Nonsense-Mediated Decay (NMD)					1	1	
1268745	Mitochondrial protein import					1	1	
1269091	Host Interactions of HIV factors					1	1	

167325	Protein processing in endoplasmic reticulum					1	1	
1269329	TNFR2 non-canonical NF-kB pathway					1	1	
1269753	G2/M Checkpoints					1	1	
1269192	Class I MHC mediated antigen processing & presentation					1	1	
83059	mTOR signaling pathway					1		1
1269203	Innate Immune System					1	1	
1269691	mRNA Splicing - Minor Pathway					1	1	
1270429	DNA Damage/Telomere Stress Induced Senescence					1	1	
1383041	Golgi-to-ER retrograde transport					1	1	
1269222	Activation of IRF3/IRF7 mediated by TBK1/IKK epsilon					1		1
PW:0000045	pentose phosphate					1	1	
790012	Biosynthesis of amino acids					1	1	
1269509	RHO GTPase Effectors					1	1	
M19613	Multiple antiapoptotic pathways from IGF-1R signaling lead to BAD phosphorylation					1		1
1269193	Antigen processing: Ubiquitination & Proteasome degradation					1	1	
83101	Vibrio cholerae infection					1		1
1268722	N-glycan trimming in the ER and Calnexin/Calreticulin cycle					1	1	

375172	Salmonella infection						1	1
P00054	Toll receptor signaling pathway						1	1
1270245	Collagen formation						1	1
1470924	Interleukin-10 signaling						1	1
1269157	Diseases associated with the TLR signaling cascade						1	1
1269156	Diseases of Immune System						1	1